Supplementary Material (ESI) for Soft Matter

Cross-linking of a charged polysaccharide using polyions as electrostatic staples

Sabyasachi Rakshit and Sanjeevi Sivasankar*

Department of Physics and Astronomy, Iowa State University, Ames, IA 50011.

Ames Laboratory, US Department of Energy, Ames, IA 50011

sivasank@iastate.edu

Supporting Information

Materials: Commercially available disodium salt of ethylene diamine tetraacetic acid (Fisher Chemicals, HPLC- grade), ethylene glycol tetraacetic acid (Fluka), calcium chloride (Fisher Chemicals), magnesium chloride (Fisher Chemicals), sodium chloride (Fisher Chemicals), sodium acetate (Fisher Chemicals) and acetic acid (Fisher Chemicals) were used as received. Milli-Q water with a resistivity of 18.2 MΩ was used for all sample preparation.

Sample preparation for force measurements: The acidic charged polysaccharide (cPS) was obtained from dew-like mucilage droplets on the leaves of the Sundew plant, *Drosera adelea*. Approximately 1 μL of the mucilage was withdrawn from the leaf using a pipette, spread on a freshly cleaned glass cover slip and dried for an hour. The sample was thoroughly rinsed with pH 5 buffer containing 50 mM EGTA and 50 mM EDTA before use. The cPS was stretched by the Si_3N_4 tip of an AFM cantilever (Olympus). Prior to use, the AFM cantilevers and glass coverslips were cleaned for 30 minutes in a 25% H_2O_2 : 75% H_2SO_4 'piranah' solution.

Single molecule force measurements: The spring constants of the AFM cantilevers were measured with the thermal fluctuation method.[1] Forces between single polysaccharide molecules were measured with an

Agilent 5500 AFM. The tip and the substrate were bought into contact for 2s and the tip was withdrawn from the substrate at a constant velocity of 1035nm/s.

Data fitting: The experimental force-extension curves without a transition were fit to a worm like chain (WLC) model,[2, 3] extended worm like chain (Ex-WLC) model,[4] freely jointed chain (FJC) model[5] and extended freely jointed chain (Ex-FJC) model.[6] Best fits were obtained with WLC and Ex-WLC models.

Table S1. Force-extension curves for experimental conditions without step-like transitions, are best fit with WLC model.

Experiment	**Number of measurements**	***Fitting standard deviation (σ)***	***Persistence length (nm)***
pH5, 1M Na^+	21	0.30	1.0±0.3
pH5, 83.1 mM Na^+	19	0.20	0.6±0.2
pH5, 1.1 mM Na^+	16	0.16	0.9±0.2
pH5, 0.23 mM Na^+	13	0.17	0.6±0.2
pH5, 0.11 mM Na^+	41	0.09	0.7±0.3
pH5, 1 mM EDTA	21	0.16	0.7±0.2
pH5, 1mM Ca^{2+}, 1mM Mg^{2+}	9	0.36	0.9±0.4
pH5, 22mM Ca^{2+}, 19mM Mg^{2+}	29	0.14	0.6±0.2
pH5,1 mM EGTA, 1 M Na^+	21	0.04	1.0±0.3
pH7, 1 mM EGTA	36	0.12	0.8±0.3
pH8,1 mM EGTA, 100 mM Na^+	12	0.14	0.6±0.2
pH 3.8,1 mM EGTA	48	0.12	1.2±0.3

The fits to WLC and Ex-WLC models were identical. The WLC model is described by the equation

$$F(z) = \frac{k_B.T}{l_p}[\frac{1}{4}(1-\frac{z}{L_c})^{-2} + \frac{z}{L_c} - \frac{1}{4}]$$

where, z is the extension, F is the force, l_p is the persistence length, L_c is the contour length, k_B is Boltzmann constant and T is the temperature. The force-extension data was first fit to the maximum unbinding force and then the fitted force range was gradually decreased until a value of l_p that varied by less that 10% was obtained. The standard deviation σ, of the WLC fitting to the force-extension curves was calculated using the equation $\sigma = \sqrt{\sum (F_{Experiment} - F_{Fit})^2 / N^2}$ where N was the total number of data points. The standard deviations for WLC fitting in different experimental conditions are given in the Table S1.

All force curves in presence of EGTA do not show step like transition events: In the presence of EGTA, not all cPS force-extension curves showed step like transition events (Table S2). Based on previous studies of polyelectrolyte chains,[7-15] it is likely that this arises because the cPS exists in both elongated and compact conformations that are long-lived and do not interchange during the experiment. Alternatively, as observed in other polyelectrolytes, the cPS might exist in a partially condensed, pearl-necklace conformation in which compact globules are separated by an extended chain.[16-20] While the compact structure can be cross-linked by EGTA, the elongated structure cannot be bridged and behaves like a simple worm like chain.

Table S2. Fraction of force curves in presence of EGTA that show step-like transitions

Experiment	Percentage (%)
pH5,1 mM EGTA	74
pH5,1 mM EGTA, 100 mM Na^+	37
pH6,1 mM EGTA	13
pH6,1 mM EGTA, 100 mM Na^+	31
pH7, 1 mM EGTA, 100 mM Na^+	16

Histogram of total length of cPS measured in single molecule force-extension experiments:

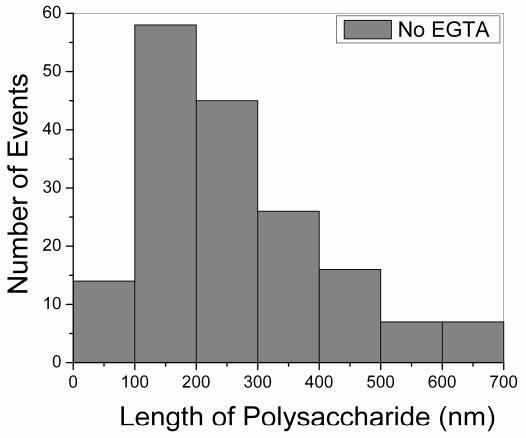

Figure S1. Distribution of total length of cPS in absence of EGTA.

Acid dissociation constant (pK_A) values of Ethylenediamine tetraacetic acid (EDTA) and ethyleneglycol tetraacetic acid (EGTA): Both ethylenediamine tetraacetic acid (EDTA) and ethyleneglycol tetraacetic acid (EGTA) are fully charged at pH 5.0. The pKA values for EDTA are,[21, 22] pK_1 = 0.0 (COOH), pK_2=1.5 (COOH), pK_3 = 2.0 (COOH), pK_4=2.69 (COOH), pK_5 = 6.13 (NH^+) and pK_6=10.37 (NH^+)

The pKA values for EGTA are,[23] pK_3 = 2.0 (COOH), pK_4=2.68 (COOH), pK_5 = 8.85 (NH^+) and pK_6=9.46 (NH^+)

Excluded Volume Calculation: The excluded volume, *X*, between two rigid segments of the cPS were calculated using the equation for polyelectrolyte excluded volume given by Fixman and Skolnick,[24]

$$X = 8l_p^2\kappa^{-1}\int_0^{\pi/2}\sin^2\theta\int_0^{w/\sin\theta}\frac{1-e^{-x}}{x}dxd\theta \qquad \text{and} \qquad w = 2\pi\beta^2 a_0\kappa^{-1}e^{-\kappa d}$$

where, β is the linear charge density, a_0 is the Bjerrum length (0.7136 nm), κ^{-1} is the Debye length (2.7 nm for 1 mM EGTA / EDTA at pH 5) and *d* is the diameter of the cPS (0.7 nm). Figure S2 shows the

distance, $X^{1/3}$, between two stiff segments of the cPS that was calculated for β values ranging from 1% cPS to 100 % cPS.

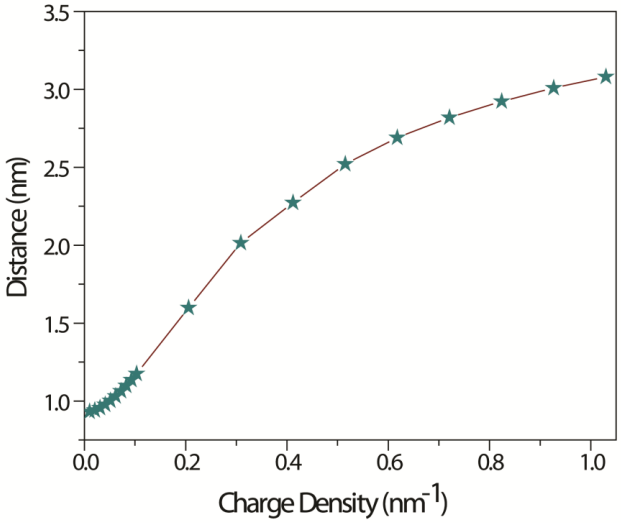

Figure S2. Distance between two stiff polyelectrolyte segments as a function of charge density.

Force-extension curves do not show conformational transitions when cPS and EGTA charges are neutralized or when the cPS charge density is increased:

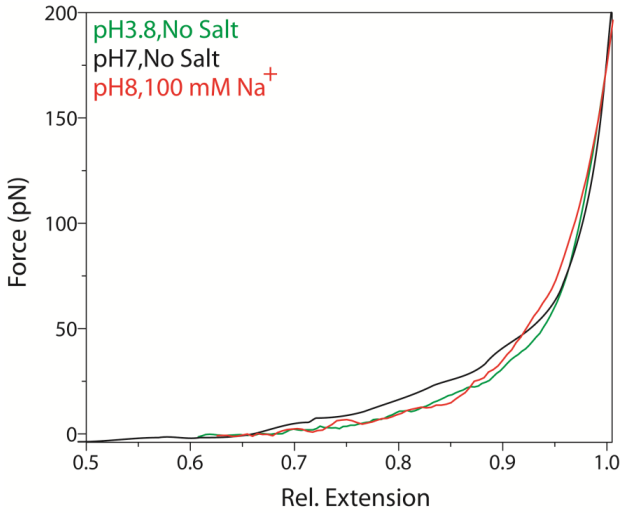

Figure S3. Normalized force-extension curves show no step-like conformational transitions when the cPS and EGTA charges are neutralized or when the cPS charge density is increased.

The electrostatic nature of the interaction between EGTA and cPS was confirmed by titrating charges on the polysaccharide and EGTA and measuring the force-extension behavior. Conformational transitions were eliminated when carboxylate groups on the cPS were neutralized at pH 3.8 (Figure S3) or when the positively charged amine groups in EGTA began to deprotonate at pH 8.0 (Figure S3). Similarly, no step-like transitions were measured when the cPS charge density was increased at pH 7.0, due to the increase in the polysaccharide excluded volume (Figure S2 and S3)

Atomic Force Microscope imaging of cPS: Polysaccharides were imaged using a multimode AFM equipped with the type J scanner and Nanoscope IIIa controller (Veeco Instruments). Tapping Mode images at a scan rate of 1.5 Hz and a drive frequency of ~310 kHz were obtained in air at ambient temperature and humidity using silicon probes with spring constant of 20-80N/m. cPS images were obtained under three conditions

(1) cPS suspended in an aqueous solution containing 22 mM Ca^{2+} and 19 mM Mg^{2+} at pH 5 were deposited on freshly cleaved mica, and incubated for one hour. Following incubation, the sample was washed with the same solution, dried overnight at ambient temperature and stored under vacuum.

(2) cPS suspended in an aqueous solution containing 50 mM EGTA at pH 5 were deposited on freshly cleaved mica, and incubated for one hour. Following incubation, the sample was washed with a solution containing 1mM EGTA at pH 5, dried overnight at ambient temperature and stored under vacuum.

(3) After images of sample *(2)* were acquired, this sample was washed with a solution containing 22 mM Ca^{2+} and 19 mM Mg^{2+} at pH 5, dried overnight at ambient temperature.

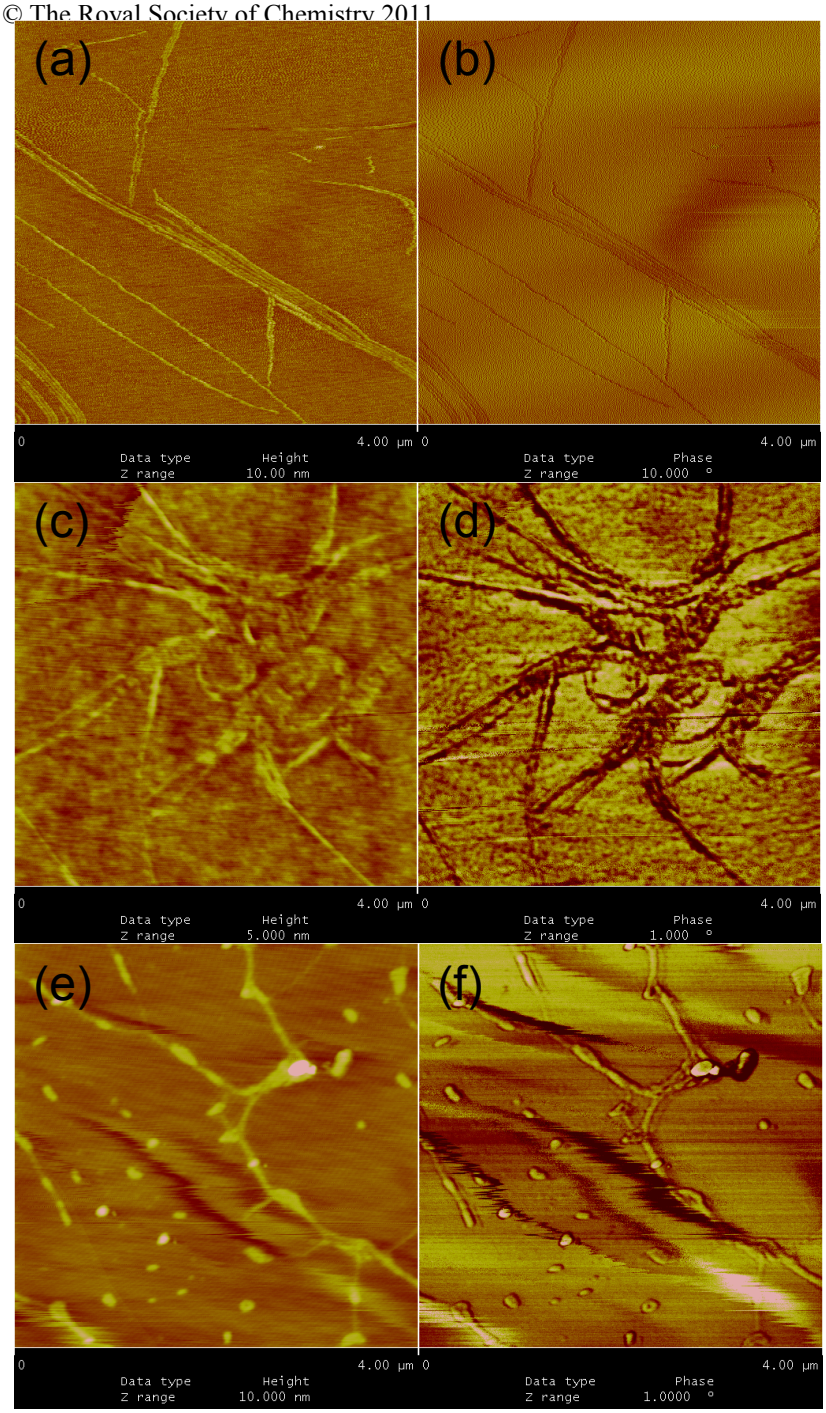

Figure S4. Height (left panels) and phase (right panels) images of cPS measured under different conditions. (a & b) cPS deposited from a solution containing divalent metal ions (Sample 1) adopt an extended conformation. (c & d) cPS deposited from a solution containing 1mM EGTA (Sample 2) show highly aggregated conformations. (e & f) When sample 2 was incubated in an EGTA free solution for one hour (sample 3), most large aggregates were eliminated and the cPS adopted a more extended conformation.

cPS deposited in the presence of divalent ions (sample 1) adopted an extended conformation, attributed to molecular combing and inhibition of subsequent chain recoil by adhesion to the mica surface (Figure S4 a & b). On the other hand, cPS deposited from a solution containing EGTA (sample 2), were highly aggregated (Figure S4 c & d). After imaging, when the aggregated cPS were incubated in an EGTA free solution for one hour (sample 3), many aggregates were eliminated and the carbohydrate adopted a more extended conformation (Figure S4 e & f). This confirms that aggregates observed in the AFM images were due to cross-linking of the cPS; as the aggregated chains were incubated in an EGTA free solution, the cross-links began to dissociate, and the aggregates began disappearing.

Force-extension behavior of the cPS in solution containing Ca^{2+} ions and EGTA: Since EGTA is routinely used as a chelating agent for divalent metal ions, we measured cPS force-extension curves in solutions containing 1 mM EGTA and 2.5mM Ca^{2+} ions.

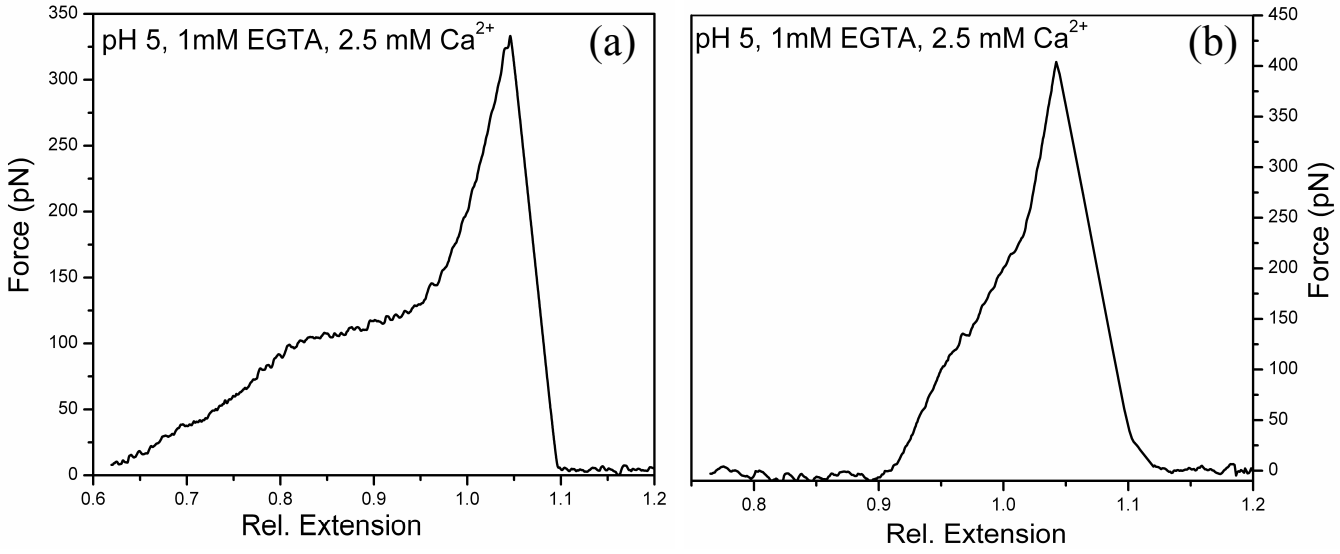

Figure S5. Normalized force-extension curves of cPS measured in solution containing 1mM EGTA and 2.5mM Ca^{2+} ions shows step-like conformational transitions.

The mucilage containing cPS was spread on a freshly cleaned glass cover slip and dried for an hour. The sample was then incubated for one hour in a pH 5 buffer containing 1 mM EGTA. The sample was then washed with a pH 5 buffer containing 1mM EGTA and 2.5 mM Ca^{2+} and incubated in the same buffer for one hour prior to the measurement. Step-like conformational transitions were observed (Figure S5), suggesting that EGTA chelated to Ca^{2+} can continue to cross-link the cPS.

Calculation of the stretching energy of the charged and uncharged polysaccharide: In order to determine if a chair to boat transition in the pyranose ring occurred during polysaccharide stretching, we used the program Spartan to calculate the conformational energy of the polysaccharide as it was stretched. The calculations were carried out using an MMFFaq force field for charged and uncharged polysaccharides with a length of four sugar monomer units, -α-D-Mannp-1,4-β-D-GlcpA-1,2-α-D-Mannp-1,4-β-D-GlcpA- (Figure S6a). At first, the ground state energy of the equilibrium conformer was estimated from a conformational search of 10000 conformers. The end-to-end distance, i.e., the distance between C4-OH of GlcpA at one end and C2-OH of Mannp at the other end, was then measured. Both polysaccharides were then gradually stretched in stepwise increments of 0.5 nm up to a maximum end-to-end distance of 22 nm. At each step, the end-to-end distance was constrained and the minimum conformational energy was calculated. The energy difference between the stretched conformers and the ground state energy is shown in Figure S6b. No chair to boat transitions was observed for both, charged and uncharged polysaccharides (Figure S6b).

A similar molecular mechanics calculation was also performed for cPS with three sugar monomer units (-β-D-GlcpA-1,2-α-D-Mannp-1,4-β-D-GlcpA-) in the presence of one Ca^{2+} ion, two Ca^{2+} ions and two Na^{+} ions (Figure S7). As expected, none of these showed a chair to boat transition.

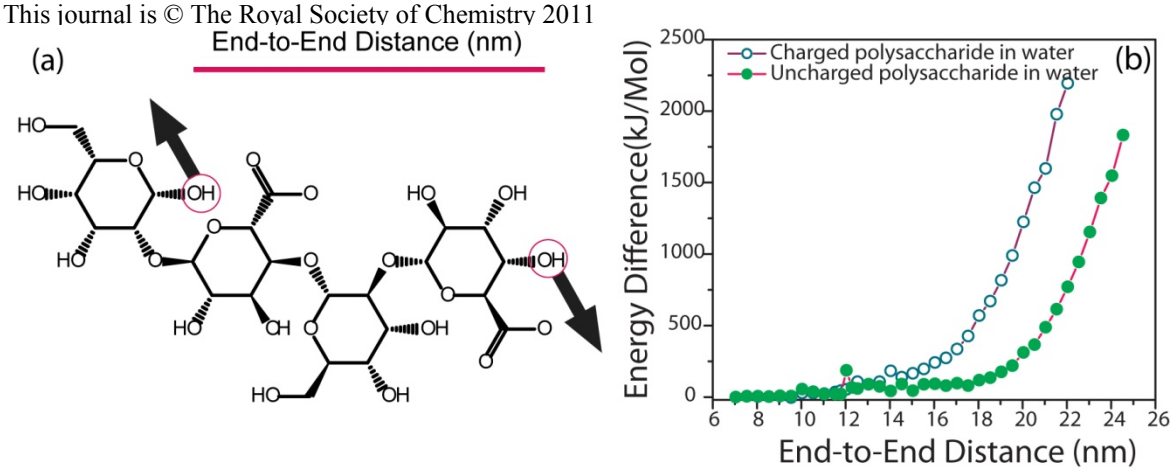

Figure S6. (a) **Polysaccharide with four sugar units showing the end-to-end distance which was increased in a stepwise fashion during the calculation. The arrows show the direction of stretching.** ***(b)*** **Energy difference between the stretched conformers and the ground state energy plotted as a function of the end to end distance.**

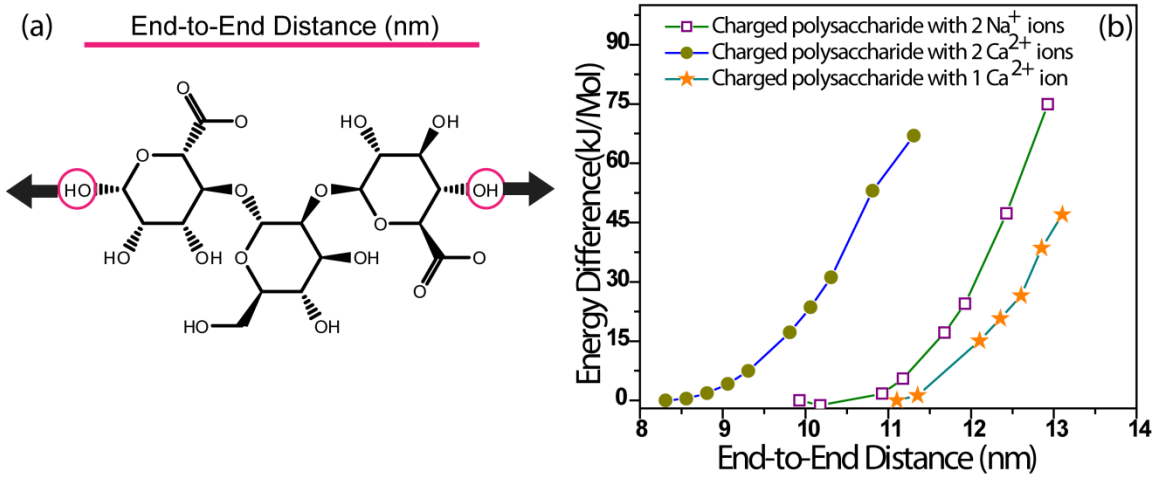

Figure S7. (a). **cPS with three sugar units showing the end-to-end distance which was increased in a stepwise fashion during the calculation. The arrows show the direction of stretching through the glycosidic linkages.** ***(b).*** **The energy difference between the stretched conformers and the ground state plotted as a function of the end-to-end distance in presence of 1 Na^{+}, 1 Ca^{2+} ion and 2 Ca^{2+} ions.**

It is possible that chair-boat transitions are not observed in these simulations because a single bond, the C1-C2 bond of α-D-mannose, bridges the two axial linkages; force is presumably transmitted only through this bond and not through the entire monomeric sugar unit.

References:

1. Hutter, J. L.; Bechhoefer, J. *Rev. Sci. Instrum.* **1993,** 64, (7), 1868.
2. Odijk, T. *Macromolecules* **1995,** 28, (20), 7016-7018.
3. Hugel, T.; Grosholz, M.; Clausen-Schaumann, H.; Pfau, A.; Gaub, H.; Seitz, M. *Macromolecules* **2001,** 34, (4), 1039-1047.
4. Wang, M. D.; Yin, H.; Landick, R.; Gelles, J.; Block, S. M. *Biophys. J.* **1997,** 72, (3), 1335-1346.
5. Smith, S. B.; Finzi, L.; Bustamante, C. *Science* **1992,** 258, (5085), 1122-1126.
6. Smith, S. B.; Cui, Y. J.; Bustamante, C. *Science* **1996,** 271, (5250), 795-799.
7. Iwaki, T.; Yoshikawa, K. *Europhys. Lett.* **2004,** 68, (1), 113-119.
8. Sakaue, T.; Yoshikawa, K. *J. Chem. Phys.* **2006,** 125, (7), 074904-6.
9. Yoshikawa, K.; Yoshinaga, N. *J. Phys.: Condens. Matter* **2005,** 17, (31), S2817-S2823.
10. Khan, M. O.; Chan, D. Y. C. *Macromolecules* **2005,** 38, (7), 3017-3025.
11. Miyazawa, N.; Sakaue, T.; Yoshikawa, K.; Zana, R. *J. Chem. Phys.* **2005,** 122, (4).
12. Noguchi, H.; Saito, S.; Kidoaki, S.; Yoshikawa, K. *Chem. Phys. Lett.* **1996,** 261, (4-5), 527-533.
13. Noguchi, H.; Yoshikawa, K. *Chem. Phys. Lett.* **1997,** 278, (1-3), 184-188.
14. Noguchi, H.; Yoshikawa, K. *J. Chem. Phys.* **1998,** 109, (12), 5070-5077.
15. Yoshikawa, K.; Takahashi, M.; Vasilevskaya, V. V.; Khokhlov, A. R. *Phys. Rev. Lett.* **1996,** 76, (16), 3029-3031.
16. Kiriy, A.; Gorodyska, G.; Minko, S.; Jaeger, W.; Stepanek, P.; Stamm, M. *J. Am. Chem. Soc.* **2002,** 124, (45), 13454-13462.
17. Kirwan, L. J.; Papastavrou, G.; Borkovec, M.; Behrens, S. H. *Nano Letters* **2004,** 4, (1), 149-152.
18. Minko, S.; Kiriy, A.; Gorodyska, G.; Stamm, M. *J. Am. Chem. Soc.* **2002,** 124, (13), 3218-3219.
19. Roiter, Y.; Oleksandr, T.; Tokarev, V.; Minko, S. *J. Am. Chem. Soc.* **2010,** 132, 13660-13662.
20. Cowman, M. K.; Spagnoli, C.; Kudasheva, D.; Li, M.; Dyal, A.; Kanai, S.; Balazs, E. A. *Biophys. J.* **2005,** 88, (1), 590-602.
21. Arthur E. Martell, R. M. S., *Critical Stability Constants*. Plenum Press: New York, 1974.
22. Harris, D. C., *Quantitative Chemical Analysis*. 7th ed.; W. H. Freeman and Company: New York, 2007.
23. Tsien, R. Y. *Biochemistry* **1980,** 19, (11), 2396-2404.
24. Fixman, M.; Skolnick, J. *Macromolecules* **1978,** 11, (5), 863-867.